ChemPubSoc Europe
DOI: 10.1002/cssc.201500375
CHEMSUSCHEM Communications

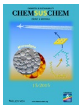

Catalytic Production of Branched Small Alkanes from Biohydrocarbons

Shin-ichi Oya,[a] Daisuke Kanno,[a] Hideo Watanabe,[b] Masazumi Tamura,[a]
Yoshinao Nakagawa,*[a] and Keiichi Tomishige*[a]

Squalane, C30 algae-derived branched hydrocarbon, was successfully converted to smaller hydrocarbons without skeletal isomerization and aromatization over ruthenium on ceria (Ru/CeO_2). The internal CH_2–CH_2 bonds located between branches are preferably dissociated to give branched alkanes with very simple distribution as compared with conventional methods using metal-acid bifunctional catalysts.

Liquid alkanes, which are important components of fuels and chemicals, are supplied by petroleum refining. Considering the diminishing reserves of crude oil, biomass, as renewable organic carbon resources, is expected to be a promising substitute.[1] The production of liquid alkanes has been attempted from lignocellulose-derived substrates such as levulinic acid, furanic compounds, and cellulose.[2–8] Some plants or microorganisms produce pure (bio)hydrocarbons, such as terpenes.[9,10] One example is squalene (2,6,10,14,18,22-hexaen-2,6,10,15,19,23-hexamethyltetracosane), high amounts of which have been reported to accumulate in *Aurantiochytrium* microalgae strains.[11,12] Typically, biohydrocarbons, in particular algae-derived ones, are large molecules with many branches. While some amount of squalene (derived from sharks) has been used in cosmetics,[11] biohydrocarbons need to be refined into smaller molecules for most other uses such as biofuel. Conventional methods for refining large hydrocarbons typically use solid acids in combination with noble-metal catalysts, and many side reactions can occur such as isomerization or coke formation.[13,14] Although isomerization is beneficial for fuel production from linear-alkane-based feedstock such as petroleum, isomerization is undesirable in the case of branched algal hydrocarbons and only complicates the reaction mixture.

Herein, we show that a Ru/CeO_2 catalyst can produce small alkanes from biohydrocarbons by regioselective C–C hydrogenolysis, without isomerization and coke formation. By using this catalyst and molecular hydrogen, internal CH_2–CH_2 bonds located between branches are preferably dissociated to give branched alkanes with very simple distributions of isomers.

First, we used *n*-hexadecane as a model substrate, to identify promising catalysts (Figure 1). Among carbon-supported catalysts (Figure 1 a–d), Ru/C showed the highest activity. The activity of Ru/C was higher than that of Ir/SiO_2 (Figure 1 e), which has been reported to be selective in hydrogenolysis of internal C–C bonds.[15–18] Ruthenium catalysts on other supports (Ru/CeO_2, Ru/SiO_2; Figure 1 f and g) were also tested, and the reaction times and catalyst amounts were adjusted to similar low levels of conversion, in order to compare selectivity. The order of activity was Ru/SiO_2 (TOF 1.8×10^2 h^{-1}) > Ru/C (79 h^{-1}) > Ru/CeO_2 (39 h^{-1}) > Ir/SiO_2 (12 h^{-1}) > Rh/C (2.8 h^{-1}) ≫ Pd/C, Pt/C (< 0.01 h^{-1}). The products were mainly *n*-alkanes for all of the tested active catalysts, and branched alkanes were hardly observed. This result is in contrast to those achieved over solid-acid catalysts, where branched alkanes are the main products through isomerization.[14,19–25] In the cases of Rh/C, Ru/SiO_2, and Ru/C, more methane and *n*-pentadecane were formed than C2–C14 alkanes, suggesting that these catalysts preferably cleave terminal C–C bonds before internal ones. In the literature, similar selectivity trends to Rh/C, Ru/SiO_2, and Ru/C catalysts have been reported for most metal-catalyzed C–C hydrogenolysis.[15,26,27] However, these trends are not desirable because the branches of algal hydrocarbons are methyl groups,

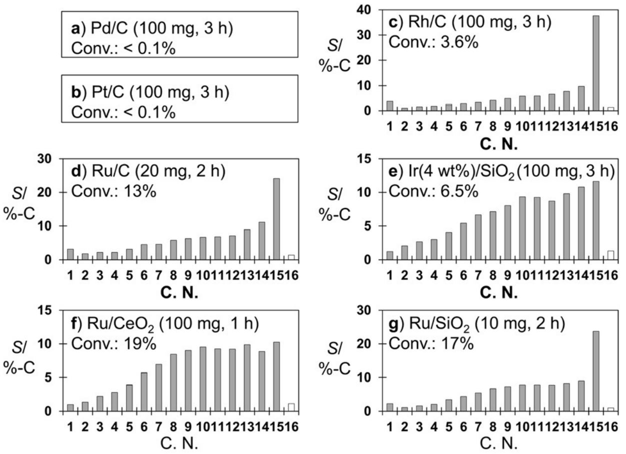

Figure 1. *n*-Hexadecane hydrogenolysis over various catalysts. Conditions: *n*-hexadecane, 2.26 g; catalyst, 10–100 mg (5 wt% metal except Ir); H_2, 6 MPa; 513 K. Gray and white bars represent linear and branched alkanes, respectively. *S*: Selectivity based on carbon, C. N.: carbon number.

---

[a] S.-i. Oya, D. Kanno, Dr. M. Tamura, Dr. Y. Nakagawa, Prof. Dr. K. Tomishige
Department of Applied Chemistry, School of Engineering
Tohoku University
6-6-07 Aoba, Aramaki, Aoba-ku, Sendai, 980-8579 (Japan)
E-mail: yoshinao@erec.che.tohoku.ac.jp
tomi@erec.che.tohoku.ac.jp

[b] Dr. H. Watanabe
Faculty of Life and Environmental Sciences
University of Tsukuba
1-1-1 Tennodai, Tsukuba, Ibaraki, 305-8572 (Japan)

Supporting Information for this article is available on the WWW under http://dx.doi.org/10.1002/cssc.201500375.

and cleavage of the terminal C–C bond removes the branch. On the other hand, on Ru/CeO_2 as well as Ir/SiO_2 the dissociation of terminal C–C bonds was not more preferable than those of other C–C bonds.

We applied Ru/CeO_2 to the hydrogenolysis of squalane (2,6,10,15,19,23-hexamethyltetracosane), which can be easily obtained by hydrogenation of squalene. Figure 2 shows GC charts of liquid samples from the reaction of squalane over Pt/H-USY and Ru/CeO_2. Pt/H-USY is a metal-acid bifunctional catalyst and was used as an example of a petroleum hydrocracking catalyst. The reaction over Pt/H-USY gave a very complex mixture of products, with >200 kinds of molecules (Figure 2 a). In literature studies of squalane hydrocracking, we noted that products are also very complex and usually analyzed roughly by boiling point.[24,28,29] On the other hand, the number of GC peaks on Ru/CeO_2 was much smaller than Pt/H-USY (Figure 2 b).

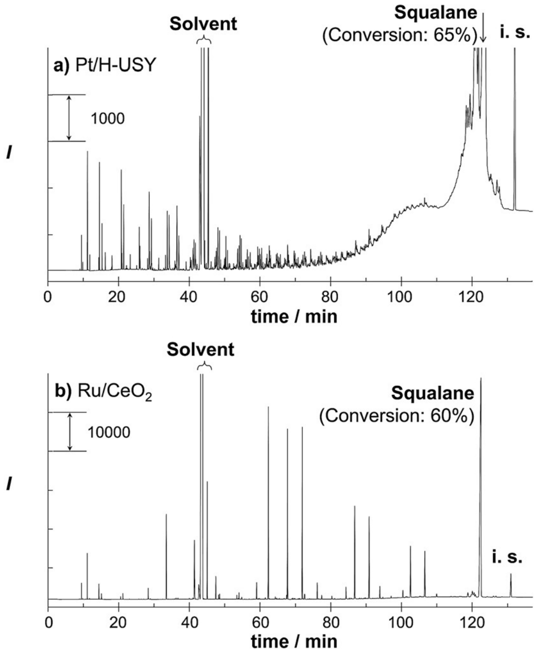

Figure 2. GC charts of liquid samples (diluted with mesitylene) of squalane hydrogenolysis. Conditions: squalane 4.23 g (10 mmol); catalyst, (a) 5.5 wt% Pt/H-USY 20 mg, (b) 5 wt% Ru/CeO_2 100 mg; H_2, 6 MPa; 513 K; (a) 3 h, (b) 6 h. *I* and i.s. represent intensity and internal standard material (*n*-octacosane), respectively.

Figure 3 shows the product distribution over Ru/CeO_2. The main products have carbon numbers of 9, 10, 14, 15, 16, 20, 21, 25, and 26. In particular, each structure with carbon number of 4, 5, 6, 9, 10, and 15 was verified by GC-MS analysis using standard samples (Supporting Information, Figure S1). All the structures of these products were substructures of squalane. The amounts of products whose formations involve isomerization was always very small. The absence of unsaturated or cyclic products was confirmed by ^1H NMR (Supporting Information, Figure S2) and GC-MS(CI). The structures of the main products indicate that the CH_2–CH_2 bonds located between the branches were selectively dissociated. The six branches in the squalane were maintained in the main products. On the other hand, Ru/SiO_2 gave products with carbon numbers below C30 (Supporting Information, Figure S3 a). The reactions at tertiary carbon, such as those giving C6–C8, C11–C13, and C17-19 products, decrease the number of branches. Hydrogenolysis of squalane over Ir/SiO_2 was also tested (Figure S3 b). The selectivity trend was intermediate between Ru/SiO_2 and Ru/CeO_2. However, the activity (TOF 2.7 h^{-1}) was much lower than those of ruthenium catalysts (Ru/CeO_2: 19 h^{-1}; Ru/SiO_2: 1.0×10^2 h^{-1}). This result agrees with literature data, reporting that iridium catalysts show very low activity towards the hydrogenolysis of branched alkanes.[18]

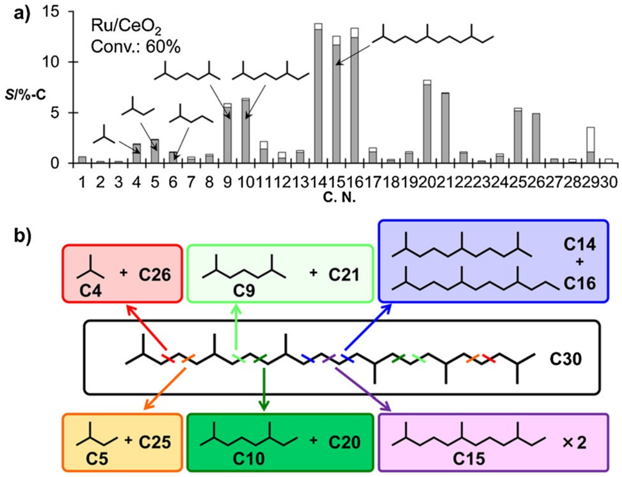

Figure 3. Squalane hydrogenolysis over Ru/CeO_2. (a) Selectivity patterns. Conditions: squalane, 4.23 g (10 mmol); Ru/CeO_2, 50 mg; H_2, 6 MPa; 513 K; 6 h. Gray bars represent the dominating isomer of products with each carbon number, and white bars represent other isomers. *S.*: Selectivity based on carbon, C.N.: carbon number. (b) Proposed C–C dissociation positions.

Figure 4 shows the time course of the hydrogenolysis of squalane over Ru/CeO_2. The product molecules became smaller at longer reaction times. The ratio of branched alkanes to *n*-al-

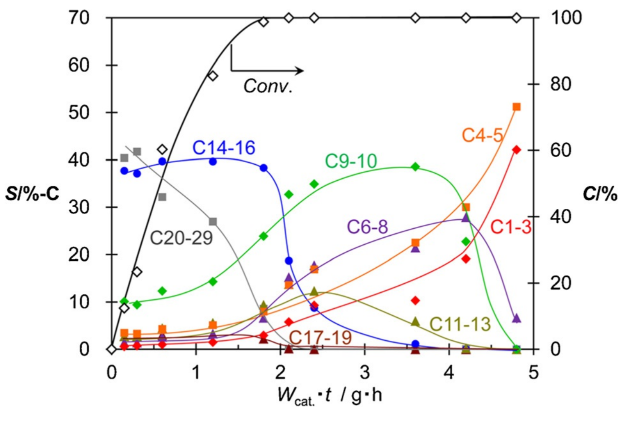

Figure 4. Reaction progress of squalane hydrogenolysis over Ru/CeO_2. Conditions: squalane, 4.23 g (10 mmol); Ru/CeO_2, 50 or 100 mg; H_2, 6 MPa; 513 K; 3–48 h. *S*: Selectivity based on carbon; *C*: conversion. W_{cat}: weight of catalyst.

kanes in ≥C4 components was always >10. When the conversion of squalane reached almost 100% (catalyst 0.1 g, time 18 h), the main products were tribranched C14–16 and dibranched C9–10. The former group can be used as components of diesel fuel or jet fuel.[30,31] A good yield of the C9–10 fraction was obtained after slightly further reaction. Further reaction gave gasoline-range (C5–C8) products. All products in this reaction were stable saturated hydrocarbons and have very low melting points because of the branches.[30,32] These properties are ideal for transportation fuels. The reaction progress of the hydrogenolysis of squalane over Ru/SiO_2 is shown in Figure S4 (Supporting Information). The selectivities to C14–16 and C9–10 on Ru/SiO_2 were not higher than 32%, and they were lower than the maximum values on Ru/CeO_2 (ca. 40%; Figure 4). These trends reflect the wider product distribution on Ru/SiO_2 compared to Ru/CeO_2.

We re-used the Ru/CeO_2 catalyst in squalane hydrogenolysis, and almost the same result was obtained as for the fresh catalyst even after 4 runs (conversion: 72%→78%→72%→75%→75%; selectivities: Supporting Information, Figure S5). Thermal gravimetric (TG) analysis of the used catalyst showed that the amount of coke formed was small (3 wt% loss from the catalyst after 5 uses; 0.02%-C of used squalane). The amount of ruthenium leaching, measured with ICP–OES, was below the detection limit (<0.5% of total ruthenium).

The Ru/CeO_2 catalyst was characterized by various techniques. The profile of temperature-programmed reduction with H_2 had a signal at 323–493 K and the area corresponded to the reduction of RuO_2 to ruthenium metal (Supporting Information, Figure S6 and Table S1). The ruthenium species in Ru/CeO_2 was reduced to Ru^0 during the reaction. The X-ray diffraction (XRD) pattern of Ru/CeO_2 did not show peaks for ruthenium metal (Supporting Information, Figure S7). The amount of H_2 adsorped onto Ru/CeO_2 was 0.9 H atoms per total ruthenium atoms (Supporting Information, Table S2). The ruthenium *K*-edge EXAFS spectrum (Supporting Information, Figure S8) could be fitted by one Ru–Ru shell with a coordination number of ~5, which is much smaller than that of the ideal hcp structure of ruthenium metal (12) and that of Ru/SiO_2 (10.5) (Table 1). These results indicate the very small size (<1.5 nm) of the ruthenium metal particles on Ru/CeO_2. In the literature, several reduced Ru/CeO_2 catalysts have been prepared for other reactions than C–C hydrogenolysis, such as CO conversions[33–35] and ammonia synthesis.[36] According to the reported characterization results, similar highly dispersed ruthenium particles (≤2 nm) were formed by reduction of ruthenium precursors supported on CeO_2. On the other hand, larger ruthenium particles were formed on other supports (<1/5 dispersion relative to Ru/CeO_2; Supporting Information, Table S2).

Table 1. Curve fitting results of Ru *K*-edge EXAFS after reduction.

Catalyst	Shells	CN[a]	*R*/0.1 nm[b]	σ/0.1 nm[c]	ΔE_0 [eV][d]	R_f [%][e]
Ru/CeO_2	Ru–Ru	4.7 (±0.6)	2.61 (±0.01)	0.097 (±0.01)	−1.10 (±1.65)	1.4
Ru/CeO_2 after reaction	Ru–Ru	5.2 (±0.6)	2.60 (±0.01)	0.083 (±0.01)	−8.35 (±1.61)	1.3
Ru/SiO_2	Ru–Ru	10.5 (±0.5)	2.66 (±0.00)	0.080 (±0.03)	−0.05 (±0.74)	0.21
Ru powder	Ru–Ru	12	2.68	0.06	0	–

[a] Coordination number. [b] Bond distance. [c] Debye–Waller factor. [d] Difference in the origin of photoelectron energy between the reference and the sample. [e] Residual factor. Fourier filtering range: 0.169–0.288 nm.

The unique selectivity of the Ru/CeO_2 catalyst might be due to the high dispersion of ruthenium metal. In fact, when Ru/CeO_2 was heated at 773 K before catalytic use to increase the particle size (ca. 2.5 nm from XRD; coordination number of Ru–Ru = 10.0 according to Ru *K*-edge EXAFS), the activity and selectivity became similar to Ru/SiO_2 (Supporting Information, Figure S9). Clarifying the mechanism that induces the selectivity requires further investigation. Preparing further small ruthenium particles might give even higher regioselectivity, which is also one target of our further studies.

Experimental Section

Carbon-supported noble-metal catalysts (Pt/C, Pd/C, Rh/C and Ru/C; 5 wt%) were purchased from Wako Pure Chemical Industries. Ru/SiO_2 and Ru/CeO_2 (Ru: 5 wt%) were prepared by impregnating SiO_2 (BET 535 $m^2 g^{-1}$) and CeO_2 (calcined at 873 K; 86 $m^2 g^{-1}$) with $Ru(NO)(NO_3)_{3-x}(OH)_x$ in HNO_3aq. Pt/H-USY (Pt: 5.5 wt%) was prepared by impregnating H-USY (Si/Al = 6.3) with H_2PtCl_6aq. Ir/SiO_2 (Ir: 4 wt%) was prepared by impregnating SiO_2 with H_2IrCl_6 aq. All the prepared catalysts were dried at 383 K for 12 h. After drying, Ru/SiO_2, Ru/CeO_2, and Pt/H-USY were heated in flowing N_2 at 573 K for 1 h. Ir/SiO_2 was calcined at 773 K for 3 h. Catalytic reaction was carried out in a 190 mL autoclave. 3.5 MPa H_2 was filled at r.t., and the pressure became 6 MPa after ~60 min heating to 513 K. The reaction time was counted after the heating. After appropriate reaction time, the reactor was rapidly cooled. Products in both gas and liquid phases were quantified with FID-GC, and qualified with GC-MS in EI and CI modes. TOF (turnover frequency; [h^{-1}]) was calculated by (increase of the total number of hydrocarbon molecules [mol])/(total number of noble metal atom [mol])/(reaction time [h]).

Acknowledgements

This work was supported by the project of Next-generation Energies for Tohoku Recovery. We thank Prof. M. M. Watanabe and Dr. M. Yoshida for providing the photos of Aurantiochytrium species for table of content. We also thank Shimadzu Corporation for GC-MS analysis.

Keywords: biomass · hydrogenolysis · metal oxides · microalgae · ruthenium

[1] a) G. W. Huber, S. Iborra, A. Corma, *Chem. Rev.* **2006**, *106*, 4044–4098; b) J. N. Chheda, G. W. Huber, J. A. Dumesic, *Angew. Chem. Int. Ed.* **2007**, *46*, 7164–7183; *Angew. Chem.* **2007**, *119*, 7298–7318; c) R. Rinaldi, F. Schüth, *Energy Environ. Sci.* **2009**, *2*, 610–626; d) A.-L. Marshall, P. J. Alaimo, *Chem. Eur. J.* **2010**, *16*, 4970–4980; e) H. Kobayashi, H. Ohta, A. Fukuoka, *Catal. Sci. Technol.* **2012**, *2*, 869–883; f) M. Besson, P. Gallezot, C. Pinel, *Chem. Rev.* **2014**, *114*, 1827–1870.

[2] a) R. Palkovits, *Angew. Chem. Int. Ed.* **2010**, *49*, 4336–4338; *Angew. Chem.* **2010**, *122*, 4434–4436; b) M. J. Climent, A. Corma, S. Iborra, *Green Chem.* **2014**, *16*, 516–547; c) Y. Nakagawa, S. Liu, M. Tamura, K. Tomishige, *ChemSusChem* **2015**, *8*, 1114–1132.
[3] G. W. Huber, J. N. Chheda, C. J. Barrett, J. A. Dumesic, *Science* **2005**, *308*, 1446–1450.
[4] R. Xing, A. V. Subrahmanyam, H. Olcay, W. Qi, G. P. van Walsum, H. Pendse, G. W. Huber, *Green Chem.* **2010**, *12*, 1933–1946.
[5] A. D. Sutton, F. D. Waldie, R. Wu, M. Schlaf, L. A. Silks, J. C. Gordon, *Nat. Chem.* **2013**, *5*, 428–432.
[6] S. Liu, M. Tamura, Y. Nakagawa, K. Tomishige, *ACS Sustainable Chem. Eng.* **2014**, *2*, 1819–1827.
[7] J. J. Bozell, G. R. Petersen, *Green Chem.* **2010**, *12*, 539–554.
[8] B. Op de Beeck, M. Dusselier, J. Geboers, J. Holsbeek, E. Morré, S. Oswald, L. Giebeler, B. F. Sels, *Energy Environ. Sci.* **2015**, *8*, 230–240.
[9] P. Metzger, C. Largeau, *Appl. Microbiol. Biotechnol.* **2005**, *66*, 486–496.
[10] T. M. Mata, A. A. Martins, N. S. Caetano, *Renewable Sustainable Energy Rev.* **2010**, *14*, 217–232.
[11] E. Naziri, F. Mantzouridou, M. Z. Tsimidou, *Lipid Technol.* **2011**, *23*, 270–273.
[12] K. Kaya, A. Nakazawa, H. Matsuura, D. Honda, I. Inouye, M. M. Watanabe, *Biosci. Biotechnol. Biochem.* **2011**, *75*, 2246–2248.
[13] M. S. Rana, V. Sámano, J. Ancheyta, J. A. I. Diaz, *Fuel* **2007**, *86*, 1216–1231.
[14] J. Weitkamp, *ChemCatChem* **2012**, *4*, 292–306.
[15] A. Majesté, S. Balcon, M. Guérin, C. Kappenstein, Z. Paál, *J. Catal.* **1999**, *187*, 486–492.
[16] a) P. T. Do, W. E. Alvarez, D. E. Resasco, *J. Catal.* **2006**, *238*, 477–488; b) M. Santikunaporn, W. E. Alvarez, D. E. Resasco, *Appl. Catal. A* **2007**, *325*, 175–187.
[17] A. Haas, S. Rabl, M. Ferrari, V. Calemma, J. Weitkamp, *Appl. Catal. A* **2012**, *425–426*, 97–109.
[18] a) D. W. Flaherty, E. Iglesia, *J. Am. Chem. Soc.* **2013**, *135*, 18586–18599; b) D. W. Flaherty, D. D. Hibbitts, E. Iglesia, *J. Am. Chem. Soc.* **2014**, *136*, 9664–9676.
[19] I. E. Maxwell, *Catal. Today* **1987**, *1*, 385–413.
[20] M. Roussel, J.-L. Lemberton, M. Guisnet, T. Cseri, E. Benazzi, *J. Catal.* **2003**, *218*, 427–437.
[21] A. Ishihara, K. Inui, T. Hashimoto, H. Nasu, *J. Catal.* **2012**, *295*, 81–90.
[22] A. Corma, A. Martinez, S. Pergher, S. Peratello, C. Perego, G. Bellusi, *Appl. Catal. A* **1997**, *152*, 107–125.
[23] M. Busto, J. M. Grau, C. R. Vera, *Appl. Catal. A* **2010**, *387*, 35–44.
[24] M. Mitsios, D. Guillaume, P. Galtier, D. Schweich, *Ind. Eng. Chem. Res.* **2009**, *48*, 3284–3292.
[25] R. de Haan, G. Joorst, E. Mokoena, C. P. Nicolaides, *Appl. Catal. A* **2007**, *327*, 247–254.
[26] F. Regali, L. F. Liotta, A. M. Venezia, M. Boutonnet, S. Järås, *Appl. Catal. A* **2014**, *469*, 328–339.
[27] C. J. Machiels, R. B. Anderson, *J. Catal.* **1979**, *58*, 268–275.
[28] K. P. de Jong, J. Zečević, H. Friedrich, P. E. de Jongh, M. Bulut, S. van Donk, R. Kenmogne, A. Finiels, V. Hulea, F. Fajula, *Angew. Chem. Int. Ed.* **2010**, *49*, 10074–10078; *Angew. Chem.* **2010**, *122*, 10272–10276.
[29] J. Francis, E. Guillon, N. Bats, C. Pichon, A. Corma, L. J. Simon, *Appl. Catal. A* **2011**, *409–410*, 140–147.
[30] T. G. Smagala, E. Christensen, K. M. Christison, R. E. Mohler, E. Gjersing, R. L. McCormick, *Energy Fuels* **2013**, *27*, 237–246.
[31] T. C. R. Brennan, C. D. Turner, J. O. Krömer, L. K. Nielsen, *Biotechnol. Bioeng.* **2012**, *109*, 2513–2522.
[32] *Diesel Fuels Technical Reviews*, Chevron Corporation. Available from http://www.chevron.com/productsservices/fuels/. (Accessed May 2015).
[33] L. A. Bruce, M. Hoang, A. E. Hughes, T. W. Turney, *J. Catal.* **1998**, *178*, 84–93.
[34] A. Satsuma, M. Yanagihara, J. Ohyama, K. Shimizu, *Catal. Today* **2013**, *201*, 62–67.
[35] X. Chen, J. J. Delgado, J. M. Gatica, S. Zerrad, J. M. Cies, S. Bernal, *J. Catal.* **2013**, *299*, 272–283.
[36] Y. Izumi, Y. Iwata, K. Aika, *J. Phys. Chem.* **1996**, *100*, 9421–9428.

Received: March 13, 2015